Relationship between Surface Morphology and Solar Conversion Efficiency of WSe_2 Photoanodes

H. J. Lewerenz,* A. Heller, and F. J. DiSalvo

Contribution from Bell Laboratories, Murray Hill, New Jersey 07974.
Received September 20, 1979

Abstract: The performance of a series of n-WSe_2 photoanodes differing in surface morphology has been investigated. A solar to electrical conversion efficiency of 3.7% is reached on a smooth photoanode in the n-WSe_2|2 M KI–0.05 M I_2|C cell. A correlation exists between the short circuit current, the open circuit voltage, and the fill factor on the one side and surface perfection, determined by scanning electron microscopy, on the other. We propose that an electric field component which parallels the layers is introduced by the steps. Because of the highly anisotropic conductivity of layered compounds the holes, on their way to the interface, are deflected and move to recombination sites at the edges of steps.

I. Introduction

Among the recent developments in materials for photoelectrochemical solar energy conversion, layered compound semiconductors have gained particular interest.[1,2] Contrary to most of the hitherto investigated semiconductors these materials show good photoanode stability in relatively oxidizing solutions. It has been suggested that this stability is due to the fact that the optical absorption near the band edge is dominated by direct transitions between hybridized metal d bands.[3,4] Since these almost intrametallic transitions leave the bonding of the illuminated semiconductor largely unaffected, the susceptibility of such electrodes to photocorrosion is low. According to Tributsch,[2] the most promising electrode materials are transition-metal chalcogenides. Upon inspection of some basic solid-state properties of these compounds, as, for instance, the metal–metal distance which determines the d–d interaction and hence also the d–d splitting, the compounds MoS_2, WS_2, WSe_2, and $MoSe_2$ appear to have particularly desirable properties.

Little appears to be known about more sophisticated but similarly important material properties that bear on solar energy conversion, such as the optical joint density of states involved in the d–d transitions and the matrix element modulation of the transition current. Some clues concerning these parameters may be obtained from visible light absorption measurements. Uncertainties exist, however, with respect to some of the basic solid-state properties in the literature,[5,6] because of differences in the growth process. This uncertainty prevents at present a rigorous theoretical analysis of the four transition-metal chalcogenides with respect to their expected solar energy conversion efficiency.

The first investigation of WSe_2 in an electrochemical environment yielded evidence that the photovoltage and photocurrent in this material are reduced by recombination losses.[7] Hence, the solar energy conversion efficiency, for a p-WSe_2 photocathode, has only been 2% and the fill factor did not exceed 0.25. It is the aim of the present investigation to characterize the causes of the losses in n-WSe_2 and to reduce these.

Tungsten diselenide crystallizes in the molybdenite structure and has the symmetry of the space group $D_{6h}^4 - P6/mmc$.[8,9] The arrangement of the tungsten atoms with respect to each other is that of a close-packed hexagonal layer. Each of these layers is surrounded by two adjacent close-packed planes containing the anions, so that the cations occupy trigonal prismatic sites. Whereas within the layers strong covalent bonding is assumed,[3,10,11] the interlayer attractive forces are due predominantly to van der Waals interaction. It is this particular bonding which gives rise to the remarkable anisotropy of this semiconductor. Depending on the growth method, WSe_2 can be either p type (iodine transport) or n type (chlorine or bromine transport). The experimental data concerning the band-gap width range between 1.35[5] and 1.57 eV.[6]

The band structure of the transition-metal compounds is determined mainly by the following:

(1) The strong overlap and covalent bonding between the metal and chalcogen s and p orbitals leads to bonding and antibonding combinations of metal–chalcogen wave functions. The resulting energy separation of the respective bands is relatively large.[10]

(2) The weaker interaction between the metal d and the chalcogen sp orbitals causes the d bands to be energetically located within the metal–chalcogen sp gap and to have relatively pure d character.

(3) The strong hybridization between the d_{z^2}, the $d_{x^2-y^2}$, and the three d_{xy}-type subbands causes an energy gap within the metal d bands. Both theoretical and experimental investigations[3,10,12] yield strong evidence that the highest occupied band has d_{z^2} character, whereas the four other d subbands are located energetically above the Fermi level. These properties are schematically illustrated in Figure 1 for the case of n-WSe_2, assuming a band gap of 1.35 eV.

II. Experimental Section

Single crystals of n-type WSe_2 were grown using chlorine transport.[13] To avoid chemical differences all samples studied were selected from a single batch. The average size of the crystal sheets was ≈0.5 cm^2 and the thickness ranged between 0.1 and 0.5 mm. The electrodes were made by covering the back of the crystals with an indium amalgam, attaching a copper wire with a conductive silver epoxy, and encapsulating in an insulating epoxy (Epoweld 3713). The electrochemical experiments were performed in the normal three-electrode potentiostatic configuration and the exposed sample surfaces were paralleling the layered structure. Accordingly, the outermost surface planes consisted of Se atoms. All potentials are referred to that of the exclusively used 2 M KI–0.05 M I_2 redox couple. The light source was a 150-W tungsten iodine lamp (Oriel Corp.). All solutions were prepared with deionized water and analytical grade chemicals.

III. Results

Upon visual inspection of the as-grown WSe_2 crystals, substantial variations in shape, thickness, and crystal morphology were found. Investigation of the samples under a light microscope revealed significant differences in surface topography. The main features found on these surfaces were (1) crack-like steps, (2) deep ruptures, (3) soft bows with obviously poor single crystalline character, (4) heaps of small, thin crystallites lying on the surface, (5) very small terraces associated with crystal growth spirals, (6) smooth concave or convex surfaces.

To study the influence of the surface morphology on the performance of the photoanode, samples with different types

0002-7863/80/1502-1877$01.00/0

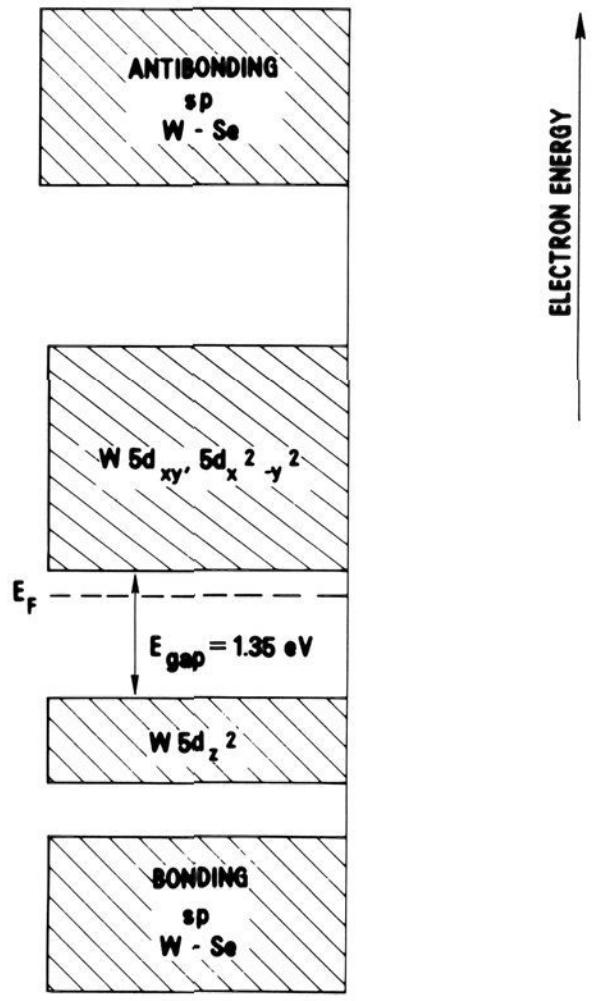

Figure 1. Schematic representation of the band structure of n-WSe_2 as extrapolated from a first-principle calculation performed on transition-metal chalcogenides.[10]

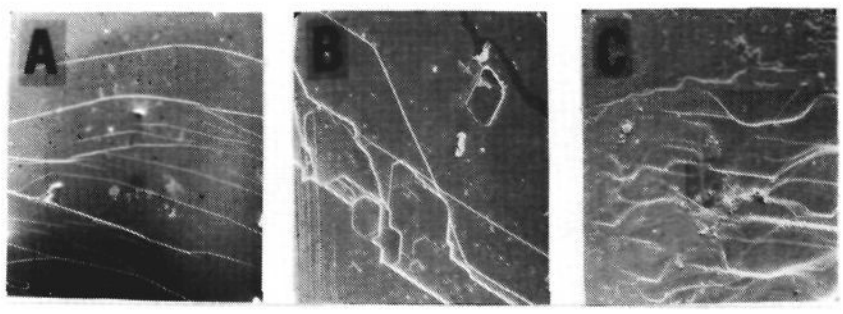

Figure 2. Scanning electron micrographs of three representative samples of n-WSe_2.

of surfaces were selected. Electron micrographs of three representative areas of these electrodes are shown in Figure 2. A difference in surface quality ranging from nearly smooth in Figure 2A through moderately structured (Figure 2B) to highly structured (Figure 2C) is noted.

For semiquantitative surface characterization, we counted the height and the length of the dislocations on each sample. This was done by taking electron micrographs at two different angles and obtaining a stereoscopic view of the surface. In addition, the height of the steps was estimated by "defocusing" under a light microscope. This method allows measurement of the step heights to within ± 2 μm. The nonhorizontal surface area was estimated to be 5% of the horizontal area in sample A (Figure 2A), 20% in sample B (Figure 2B), and 80% in sample C (Figure 2C).

The power output characteristics of photoanodes made with samples A, B, and C are shown in Figure 3. Drastic differences in cell performance are observed. The short circuit current, the open circuit voltage, and the fill factor decrease markedly from the smoothest electrode (sample A) to the most structured one (sample C). Sample A has a fill factor of 0.37 and a maximum power point at 0.35 V. Sample B has an open circuit voltage of 0.5 V and a fill factor of 0.25 and its normalized short circuit current is 40% of that of sample A. Sample C has an open circuit voltage of 0.39 V and a fill factor of 0.23 and its normalized short circuit current is only one-third of that of sample

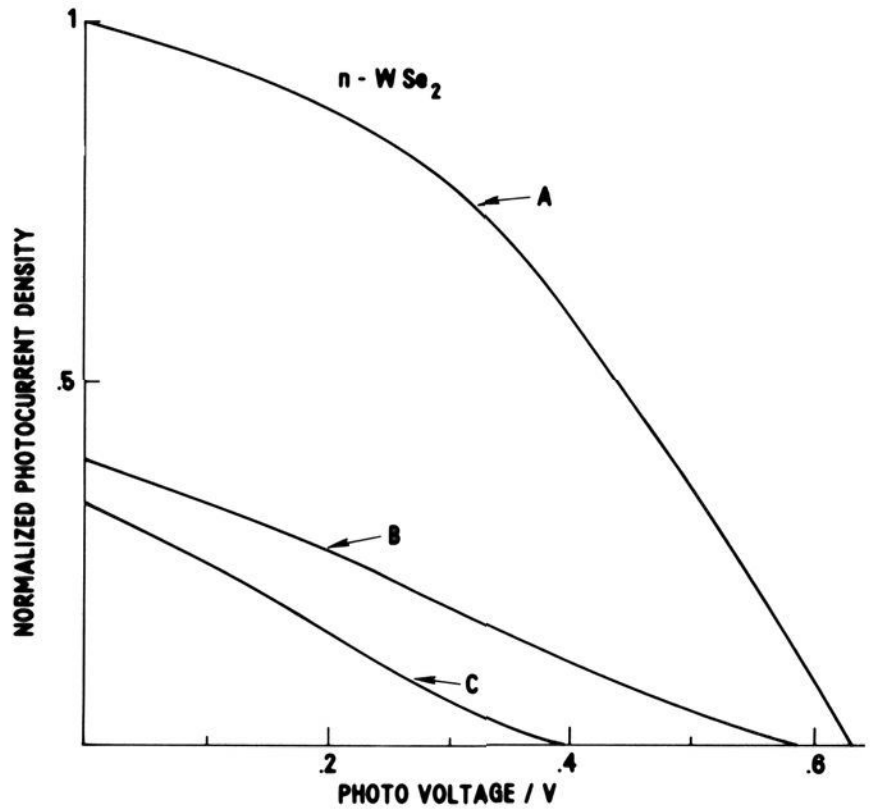

Figure 3. Current–voltage characteristics of the samples shown in Figure 2 in a 2 M KI–0.05 M I_2 solution; the solution was exposed to air.

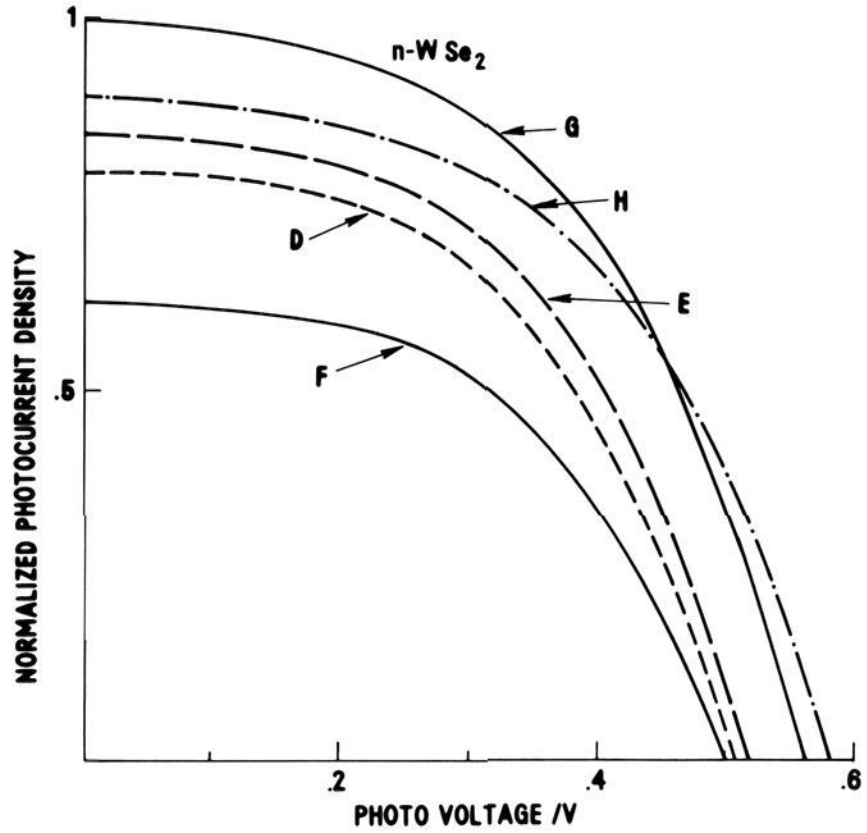

Figure 4. Current–voltage characteristics of five samples with good surface quality; solution, 2 M KI + 0.050 M I_2; air.

A. Observations on additional electrodes indicate a similar correlation between surface quality and photoanode performance.

Consequently, we selected by microscopy additional samples whose surfaces appeared to be "smooth". The current–voltage characteristics of these are shown in Figure 4. These samples, labeled D–H, exhibit fill factors as high as 0.5, the highest for any semiconductor–liquid junction cell with a layered compound photoanode. The electron micrographs of samples D, E, and H are shown in Figure 5. The short-circuit current density of sample F, with some surface structure, is slightly lower than that of the other electrodes.

In order to get an estimate of the solar conversion efficiency, the performance of electrode D has been measured in sunlight. The result, obtained at an irradiance of 92.5 mW/cm^2, is shown in Figure 6. The maximum power point is at 0.33 V, and at 10.7 mA/cm^2, with a resulting solar conversion efficiency of 3.7%. As is evident from Figure 4, some samples show better

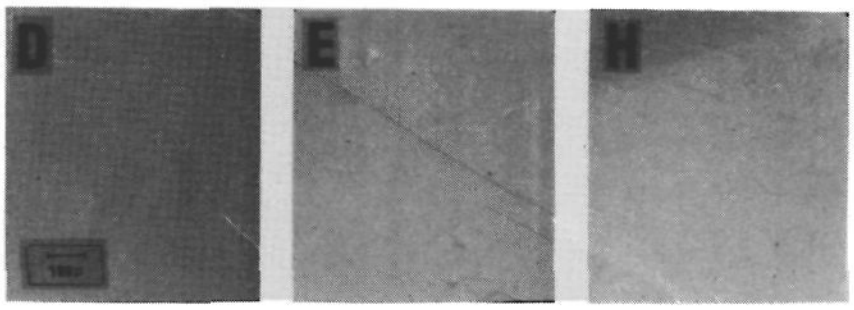

Figure 5. Scanning electron micrographs of the three n-WSe_2 samples (D–H) whose solar cell performance is shown in Figure 4.

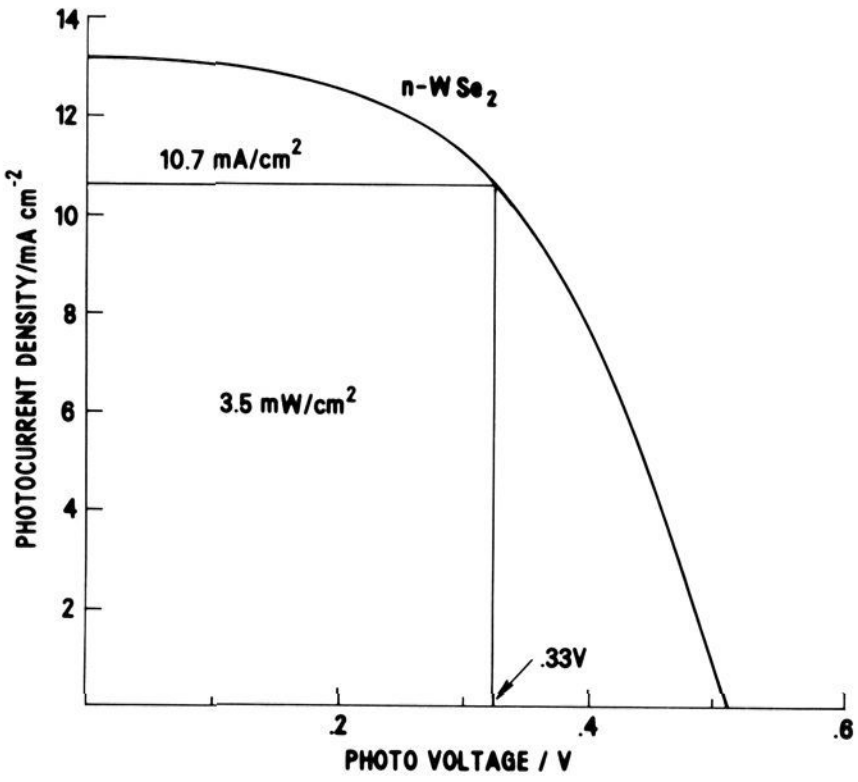

Figure 6. Current–voltage characteristics of photoanode D (see also Figures 4 and 5) under 92.5 mW/cm² sunlight in the n-WSe_2|2 M KI–0.05 M I_2|C cell.

overall performance than sample D. The best of these, sample G, the surface of which was accidentally damaged before being measured in the sun, had a maximum power output which exceeded that of electrode D by a factor of 1.4, bringing the estimated solar conversion efficiency to 5.2%.

In other semiconductors, it has been shown that recombination sites at or near the surface change the short circuit photocurrent spectra in three respects: the current (quantum) efficiency decreases at all wavelengths, the relative short wavelength response drops, and under intense illumination (with a laser beam) the current efficiency declines further.[14,15] Figure 7 shows the photocurrent spectra of two parts of the same n-WSe_2 photoanode. The top spectra are those of a relatively smooth part of the electrode and the bottom of a highly structured part. It is seen that the effect of structure on the surface is to reduce the overall current efficiency, to lower the relative response at short wavelengths, and to cause a drastic drop in current efficiency under intense illumination ("laser on"). The enhanced recombination probability under intense illumination has been explained by the increased steady-state concentration of both electrons and holes in the region which is depleted in the majority carriers (electrons).[14] In Figure 7 the spectra with the "laser on" were measured at an irradiance of 2 mW/cm² at 6328 Å. While such irradiance causes practically no decline in quantum efficiency on the smoother part of the photoanode, the quantum efficiency at the structured part is reduced by a factor of ≈20.

IV. Discussion

The comparison of the electron micrographs in Figures 2 and 5 and the respective current–voltage characteristics (Figures 3 and 4) reveals a striking relationship between surface quality and cell performance. Since most of the observed surface features result in steps, we shall proceed to examine the role of such steps in layered semiconductors.

First, we consider the ideal case of a layered semiconductor with a smooth surface (Figure 8a). The creation of electron–hole pairs by light absorption within the depletion layer is

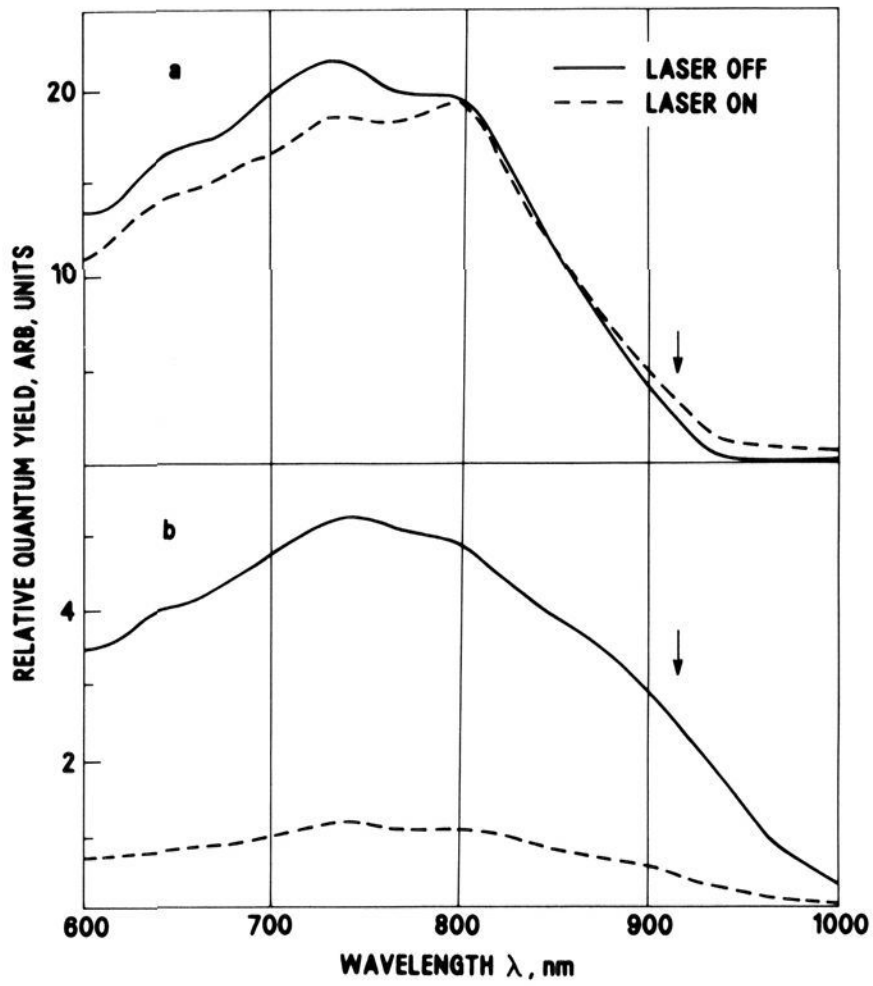

Figure 7. Photocurrent spectra of two parts of the same n-WSe_2 photoanode: (a) relatively smooth part; (b) heavily structured part. The arrows mark the band edge. The solid lines represent the relative current yields at very low levels of illumination. The dashed lines represent the relative yields when the sample is flooded with 2 mW/cm² of 6328-Å light. The spectra are corrected for the response of the system. Note the fourfold decline from (a) to (b) and the further fivefold decline in (b) (but not in (a)!) upon flooding with 6328-Å light.

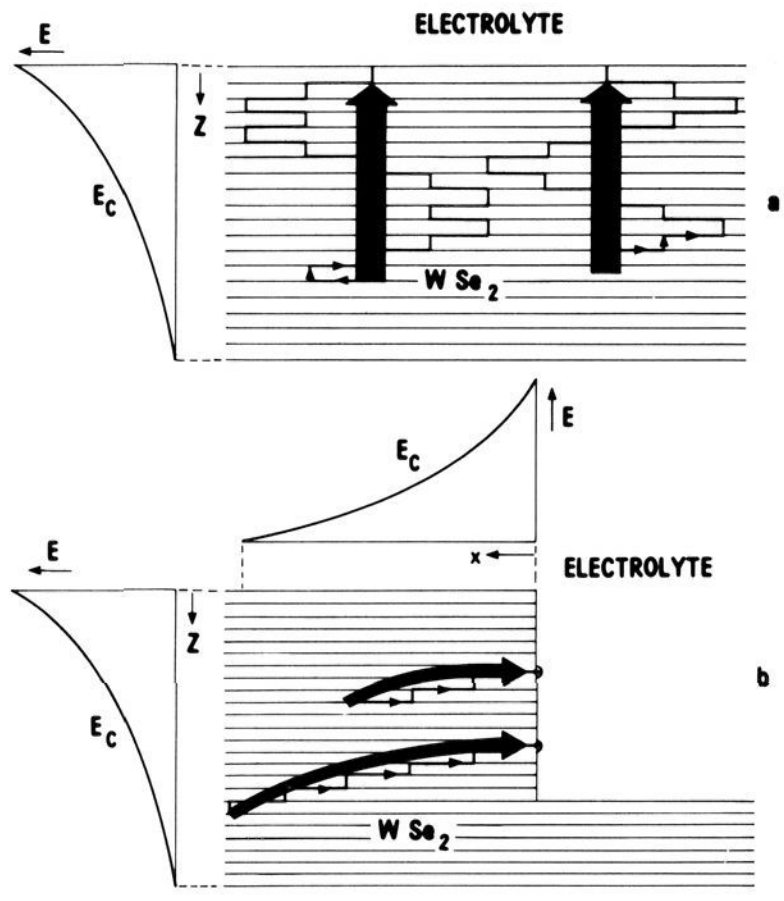

Figure 8. Schematic representation of trajectories of minority carriers: (a) for an ideal smooth surface in contact with an electrolyte; (b) for a surface with a step exposed to the electrolyte.

followed, as usual, by transport of minority carriers to the surface. In layered compounds, however, mobility within the layers is high, while mobility perpendicular to the layers is low. Most of the charge transport in the perpendicular direction appears to be determined by randomly distributed stacking faults, introducing an extrinsic conduction mechanism.[16] The presence of stacking faults causes pronounced effects on transport, since translational invariance is systematically destroyed in the direction perpendicular to the layered structure. Thus, real crystals of layered semiconductors may be viewed as one-dimensional disordered systems with extrinsic conduction paths parallel to the *c* axis.

The pronounced anisotropy of the electrical conductivity in layered compounds[3,5] suggests that the charge carriers move, on their way to the surface, predominantly within the layers, i.e., parallel to the main surface as schematically shown in Figure 8 (in which the relative path of the charge carriers within the layers is compressed). The random character of interlayer charge transport due to extrinsic conduction leads to a variety of possible paths, two of which are represented in Figure 8a.

The presence of a step on the surface introduces two significant changes. First, in contrast to a smooth surface which does not exhibit unsaturated bonds in the direction perpendicular to the surface, strong covalent bonds are exposed to the electrolyte at the edge of a step. Thus, there is a high probability that species from the environment will be chemisorbed on the edge or that this surface of WSe_2 will be otherwise changed to saturate the otherwise dangling bonds. The new compositions on the edge introduce new surface states, some of which appear to be located in the semiconductor band gap.[17] These are recognized recombination sites and shunts in solar cells, known to reduce fill factors and open circuit voltages.[18,19]

Second, the exposure of a step to the redox couple solution results in a space charge region parallel to the layers. The depth of this region will not be very different from the one at an ideal surface since the static dielectric constants for the two directions differ only by a factor of about 2.[20] However, charge carriers created within the depletion region parallel to the layers will drift toward the edge of the step in the acting electric field. A step may thus be regarded as a collector of minority carriers which otherwise would have reached the surface that parallels the layers in the semiconductor. In a simplified picture, this deflection of carriers is seen in Figure 8b. Once the minority carriers reach the edge of a step, most of them recombine because of the high density of surface states.

In summary, the reduction in current efficiency (which is particularly pronounced under intense illumination), the enhanced loss in photocurrent efficiency at wavelengths below 800 nm which are absorbed nearer to the surface, and the subband gap response ($\lambda > 917$ nm) in the photocurrent spectrum of the structured surface (Figure 7) all point to the presence of surface or near-surface states that are introduced with surface structure. The drastic decrease in photocurrent, photovoltage, and fill factor (Figures 3 and 7) is explained by the drift of minority carriers near faults to the edges of the step which are rich in surface states and on which recombination is likely.

The model presented indicates that in layered semiconductors surface damage is of extreme importance to all solar cells, including semiconductor–liquid junction, Schottky, and other devices. The regions defined by the penetration of the depletion layer in the direction parallel to the layers (at a step) might be considered as essentially "dead" in that their photoresponse is negligible. The model predicts that the efficiency obtained with flat single crystalline surfaces will be markedly enhanced.

The future invention of chemical methods to reduce high recombination rates on planes parallel to the *c* axis, in a manner analogous to those employed in the case of n-GaAs surfaces,[17,18] may further improve the efficiency of these cells and open the way to the use of polycrystalline layered chalcogenide semiconductors in semiconductor–liquid junction and other solar cells.

Acknowledgments. We thank B. Miller, M. Schluter, and S. Menezes for enlightening discussions and S. D. Ferris for the electron micrographs.

References and Notes

(1) H. Tributsch, *Ber. Bunsenges. Phys. Chem.*, **81**, 4, 361 (1977).
(2) H. Tributsch, *Z. Naturforsch. A*, **32**, 972 (1977).
(3) J. A. Wilson and A. D. Yoffe, *Adv. Phys.*, **18**, 193 (1969).
(4) M. G. Bell and W. Y. Liang, *Adv. Phys.*, **25**, 1, 53 (1976).
(5) L. C. Upadhyayula, J. J. Loferski, A. Wold, W. Giriat, and R. Kershaw, *J. Appl. Phys.*, **39**, 10, 4736 (1968).
(6) R. F. Frindt, *J. Phys. Chem. Solids*, **24**, 1107 (1963).
(7) J. Gobrecht, H. Gerischer, and H. Tributsch, *Ber. Bunsenges. Phys. Chem.*, **82**, 1331 (1978).
(8) R. Kershaw, M. Vlasse, and A. Wold, *Inorg. Chem.*, **6**, 8, 1599 (1967).
(9) J. Monzack and M. H. Richman, *Metallography*, **5**, 279 (1972).
(10) L. F. Mattheiss, *Phys. Rev. B*, **8**, 8, 3729 (1973).
(11) R. M. White and G. Lucovsky, *Solid State Commun.*, **11**, 1369 (1972).
(12) R. S. Title and M. W. Shafer, *Phys. Rev. Lett.*, **28**, 13, 808 (1972).
(13) H. Schafer in "Chemical Transport Reactions", Academic Press, New York, 1964, p 57.
(14) A. Heller, K. C. Chang, and B. Miller, *J. Am. Chem. Soc.*, **100**, 684 (1978).
(15) K. C. Chang, A. Heller, and B. Miller, *J. Electrochem. Soc.*, **124**, 5, 697 (1977).
(16) R. Fivaz and Ph. E. Schmid in "Physics and Chemistry of Materials with Layered Structures", Vol. 4, P. A. Lee, Ed., D. Reidel, Holland, 1976.
(17) S. M. Ahmed and H. Gerischer, *Electrochim. Acta*, **24**, 705 (1979).
(18) B. A. Parkinson, A. Heller, and B. Miller, *J. Appl. Phys.*, **33**, 521 (1978).
(19) B. A. Parkinson, A. Heller, and B. Miller, *J. Electrochem. Soc.*, **126**, 954 (1979).
(20) K. Zeppenfeld, *Opt. Commun.*, **1**, 377 (1970).